Available online at BCREC website: https://bcrec.id

Bulletin of Chemical Reaction Engineering & Catalysis, 17 (4) 2022, 882-893

Research Article

Performance of CdS/TNTAs Nanocomposite in Removing Ciprofloxacin and Hydrogen Production Using Simultaneously Electrocoagulation-Photocatalysis Process

Rahayu Lestari Sugihartini[1], Reno Pratiwi[1,2], S. Slamet[1,*]

[1]Chemical Engineering Department, Universitas Indonesia, Depok, 16424, Indonesia.
[2]Petroleum Engineering Department, Universitas Trisakti, Jakarta, 11440, Indonesia.

Received: 14th November 2022; Revised: 24th December 2022; Accepted: 25th December 2022
Available online: 26th December 2022; Published regularly: December 2022

Abstract

This study used CdS as a pair of TiO_2 Nanotube Arrays (TNTAs), considering the position and width of the energy band gap, which is expected to increase photocatalyst performance. The nancomposite was synthesized using the successive ionic layer adsorption reaction (SILAR) method, with $Cd(CH_3COO)_2$ and Na_2S as precursors. The CdS/TNTAs nanocomposite is expected to reduce the energy band gap to enable the visible and UV spectrum to activate the photocatalyst. Additionally, the formed heterojunction mechanism provides opportunities for the trajectories of electrons and holes to be farther apart and reduce the recombination rate. The degradation ability of CdS/TNTAs nanocomposite in the photocatalytic process was evaluated using samples of ciprofloxacin liquid waste as an antibiotic, which is quite challenging to decompose completely. The ability of the photocatalytic process to produce hydrogen gas was also observed and its performance synergized with the electrocoagulation process. The result showed that the use of CdS as a TNTAs partner in CdS/TNTAs nanocomposites affects increasing photocatalyst performance, both in degrading ciprofloxacin and producing hydrogen gas. Furthermore, the CdS/TNTAs nanocomposite increased the photocatalytic process's ability to degrade ciprofloxacin and produce hydrogen from 8.5 to 20.5% and 6 to 23.5 μmol/m^2 compared to using TNTAs alone. The processing capability is further enhanced when run in synergy with the electrocoagulation process where the removal of ciprofloxacin reaches 86.55% and the hydrogen produced is 2.62×10^6 μmol/m^2.

Keywords: CdS/TNTAs; Ciprofloxacin Degradation; Electrocoagulation; Hydrogen Production; Photocatalysis

How to Cite: R.L. Sugihartini, R. Pratiwi, S. Slamet (2022). Performance of CdS/TNTAs Nanocomposite in Removing Ciprofloxacin and Hydrogen Production using Simultaneously Electrocoagulation-Photocatalysis Process. *Bulletin of Chemical Reaction Engineering & Catalysis*, 17(4), 882-893 (doi: 10.9767/bcrec.17.4.16435.882-893)

Permalink/DOI: https://doi.org/10.9767/bcrec.17.4.16435.882-893

1. Introduction

The presence of antibiotic pollutants in waters can increase bacterial resistance to antibiotics [1], thereby potentially endangering human health[2]. Ciprofloxacin (CIP) is an antibiotic used to treat various types of infections, and when consumed, it undergoes partial metabolism hence the rest is excreted into the environment and detected in various environmental matrices [3]. Sanseverino *et al.* [4] stated that CIP is one of the antibiotics found in high concentrations in various water (>10 ng/L).

Advance Oxidation Processes (AOPs) are considered to have a good performance in degrading antibiotics. Photocatalysis is one of the developed AOPs technology with a significant ability to degrade organic pollutants, in addition to its

* Corresponding Author.
Email: slamet@che.ui.ac.id (S. Slamet)

simple and low-cost process. TiO_2 was widely selected in the design of this technology due to its strong oxidizing ability, economical price, non-corrosiveness, non-toxic, and abundance in nature [4–6]. The reduction reaction in the photocatalyst produces hydrogen gas in aqueous solutions; hence it acts as an alternative energy source. However, there are several obstacles to TiO_2, such as the high recombination rate, which reduces the efficiency of the redox reactions in the electrons and holes formed during the process [7]. Another condition is the large energy band gap (3 – 3.2 eV), which indicates that the TiO_2 photocatalyst can only be active on irradiation using light in the UV spectrum range [5]. Several studies have been conducted to improve the performance of TiO_2 in the photocatalyst process, such as by changing the surface morphology capable of increasing the contact area of the immobilized photocatalyst [8–10]. Other methods include metal or non-metal doping, dye sensitization, co-catalysts, or coupling with other semiconductors with narrower bandgap energy to form TiO_2 nanocomposites [6,11,12]. These ways increase its photocatalytic activity by broadening the light absorption ability towards visible light. Moreover, this process also increases the separation efficiency between electrons and photogenerated holes [6,13].

In our previous research, we tested the effectiveness of the TiO_2 photocatalyst with the morphology of the immobilized titania nanotube array (TNTAs) in the photocatalyst process of dye waste[14]. The nanotube array morphology increases surface area and irradiation effectiveness and can suppress the recombination rate between electrons and holes [14]. Subsequently, a study by Pelawi *et al.* [15] improved the performance of TiNTAs by depositing CuO as an electron trapper and providing a smaller energy band gap of the photocatalyst. In another study, adding Fe as a dopant was also tried, which gave an improved photocatalyst performance effect [16,17]. Both modifications successfully suppressed the electron-hole pair recombination rate and became more responsive to visible light exposure.

Efforts to increase the efficiency of the waste treatment process can be made by combining several alternative processes sequentially or simultaneously through the photocatalysis process with electrocoagulation. According to Ahmadzadeh *et al.* [18], electrocoagulation is an efficient method of removing dissolved pollutants that involves an electrochemical reaction with aluminum or iron electrodes as anodes and stainless steel as cathodes. This process produces a coagulant from the oxidation of aluminum or iron capable of adsorbing dissolved pollutants. At the same time, the production of hydrogen gas occurs from the reduction of H^+ ions by electrons on the cathode surface. The disadvantage of this method is that the processing of pollutants is limited to removing their contents, and the hazardous nature of toxins is not eliminated from the waste. Furthermore, the separation process using electrical resources results in an expensive electrocoagulation process [19].

The combination of photocatalytic processes with electrocoagulation has been carried out in several studies. In a sequential combination of processes, the electrocoagulation sequence followed by photocatalysis combined solute removal efficiency of more than 90% [20]. Meanwhile, in the reverse order, photocatalysis followed by electrocoagulation, lower efficiency was obtained [21]. A preliminary study on photocatalysis and electrocoagulation was conducted simultaneously in one reactor. Research by Sharfan *et al.* [14], Pelawi *et al.* [15], and Muttaqin *et al.* [16] tested the combined performance of photocatalysis and electrocoagulation processes simultaneously. It gave much better results regarding dissolved pollutant removal and hydrogen gas production.

In this study, the modification of TiO_2 photocatalysts was done differently by using immobilized TiO_2 (TNTAs) combined with CdS semiconductors to form photocatalyst nanocomposites. The position and value of the energy band gap of CdS which is more responsive to visible light, are used to increase the photocatalyst ability of the CdS/TNTAs nanocomposite. The heterojunction mechanism reduces the rate of electron-hole recombination and widens the spectrum of light capable of activating photocatalysts [22,23]. The SILAR method was used in synthesizing nanocomposites by considering the easy process, with minimal energy requirements and a pretty good deposit capability. XRD, UV-Vis DRS, FESEM, and EDX characterizations were made on the synthesis of nanocomposites to validate crystallinity, energy band gap, morphology, and the presence of appropriate components.

Efforts to optimize the process are also carried out by combining photocatalysis and electrocoagulation simultaneously to determine how to improve the process performance significantly. The similarity of electrocoagulation and photocatalysis in their ability to remove dissolved pollutants while producing hydrogen has beneficial and optimization effects when carried out simultaneously. The effect of con-

ducting both processes was observed and measured to determine their ability to remove dissolved ciprofloxacin and produce hydrogen gas. The process of merging both processes is likely to increase performance and act as an alternative waste treatment process that is effective, environmentally friendly, and cost-effective.

2. Materials and Methods

2.1 Preparation of TNTAs and Synthesis of CdS/TNTAs

Ti plates (8.0 cm × 4.0 cm × 0.1 cm) were purchased from Shaanxi Yunzhong Metal Technology Co. LTD. They were first polished mechanically with sandpapers (1500 CW) before utilizing the chemical process in a solution containing HF, HNO_3, and distilled water (1:3:46 volume based) for two minutes. The polished Ti plate was then rinsed with distilled water and sonicated for five minutes to remove all impurities. Next, the anodization process was carried out in a beaker glass using glycerol 98% as an electrolyte containing NH_4F 0.5 wt%, 25 %(v/v) of distilled water and constantly stirred for 2 hours. Ti plate was used as an anode, Pt as the cathode at a fixed potential of 50V, and powered using a CD power supply for 2 hours. For the anodization, TiNTAs were rinsed with distilled water to remove excess glycerol, dried at room temperature, and then stored in a desiccator.

The SILAR method used $Cd(CH_3COO)_2$ and Na_2S as precursors to form CdS/TNTAs nanocomposites. The Cd^{2+} and S^{2-} concentrations varied at 0 M, 0.05 M, 0.1 M, and 0.2 M in an aqueous solution with the prepared TiNTA plates immersed in Cd^{2+} solution for 5 minutes, then rinsed with water to remove excess Cd^{2+}. Furthermore, the plate was immersed in a solution of S^{2-} for 5 minutes and rinsed with water to remove excess S^{2-}, thereby completing a single SILAR deposition cycle. This process was repeated for six cycles based on the study of the optimal conditions for the synthesis of CdS/TiO_2 nanocomposites [24]. By varying the concentration of the precursors using composite values of 0 M, 0.05 M, 0.1 M, and 0.2 M, composite samples with different CdS contents were obtained and denoted as T, CT 0.05, CT 0.1, and CT 0.2, respectively.

2.2 Sample Characterization

The morphology of the photocatalyst was investigated using FESEM-EDX comprising Thermo Scientific – Quatro S in high vacuum mode with 20,000 magnification, a spot size of 4.0, 15 kV voltage, and mapping EDX mode. The crystallite formation was observed using an x-ray diffractometer (Empyrean Series 3 – Panalytical) at voltage and current rates of 40 kV and 30 mA current using Cu anode (Kα = 0.15406 nm). The optical properties of the photocatalyst and gap energy were measured and calculated using the UV-Vis diffuse reflectance spectroscopy (Harrick Scientific Agilent Cary 600 UV-Vis DRS) and the Kubelka-Munk method.

2.3 Electrocoagulation-Photocatalytic Activity Test

An electrocoagulation activity test was carried out in a reactor vessel containing a 500 mL ciprofloxacin (CIP) concentration of 10 ppm at pH 10. The reactor was equipped with an aluminum plate of 10 cm × 4 cm × 0.1 cm as the anode and stainless steel 316 plates of 2.5 cm × 8 cm × 0.1 cm as the cathode with a distance of 1.5 cm and each of which is connected to a DC generator (Zhaoxin RXN-605D, 60 V, 5 A). The reactor was placed in a box full of reflectors, and the combined system of electrocoagulation-photocatalysis was tested in the same reactor by adding a photocatalyst plate on the opposite side of 8 cm × 4 cm × 0.1 cm to the system, as shown in Figure 1. The reactor was well isolated, and the hydrogen produced

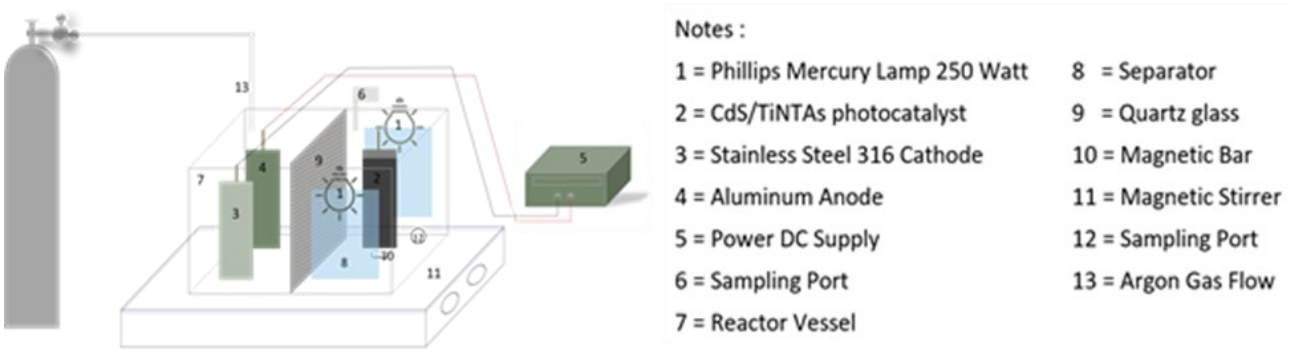

Figure 1. Experimental set-up of electrocoagulation-photocatalysis.

was measured every 60 min using a 1 mL Hamilton syringe, while the decrease in the solution concentration was also investigated every 60 min. During the performance test, the solution was stirred continuously while being exposed to illumination from two mercury lamps consisting of 17.25% UV, 82.75% visible light, and 250 W. Before each experiment, argon gas is flown through the reactor for 5 min to remove oxygen from the system.

Ciprofloxacin removal was measured by taking the solution sample every 60 min and observed using UV-Vis Spectrophotometer (Shimadzu, UV Mini 1240). The measurement was conducted around 272 nm, with the decrease in ciprofloxacin concentration measured using the following equation:

$$Removal\ Efficiency\ (\%) = \frac{C_0 - C}{C_0} \quad (1)$$

where C_0 and C denote the concentration of CIP in mg/L (ppm) at the initial and at a particular time, respectively. The hydrogen produced from the combined system of electrocoagulation-photocatalysis was analyzed every hour using a Gas Chromatography (Shimadzu GC-8A) system equipped with a Molecular Sieve (MS) Hydrogen 5 A column, with a known retention time for argon as the gas carrier.

3. Results and Discussion

3.1 FESEM-EDX Characterization

FE-SEM/EDX characterization determines the morphology and elemental composition of the modified photocatalyst surface. Figure 2 shows the images of T, CT0.05, CT0.1, and CT0.2 with TiO_2 in nanotubular shapes and self-organized. The tube diameters vary due to the inconstant stirring with EDX characterization used to confirm the formation of CdS/TNTAs.

Table 1 contains information about the elemental composition at the photocatalyst surface. It shows that the mass ratio of Cd increases with the rise in the amount of Cd added to the TiO_2 photocatalyst. Therefore, it can be concluded that the synthesized composite was high in Cd, also known as Cd-rich. It is common when the composite is synthesized via a solution-based phenomenon. This condition is usually due to titania's isoelectric point at pH

Table 1. Elemental composition on the photocatalyst surface.

Photocatalyst	% Component Mass				
	Ti	O	C	Cd	S
T	60.7	37.1	2.2	0	0
CT 0.05	53.2	38.6	3.4	1.8	0.1
CT 0.1	56.8	34.7	2.1	4.1	0.3
CT 0.2	52.3	35.5	4.4	4.7	0.4

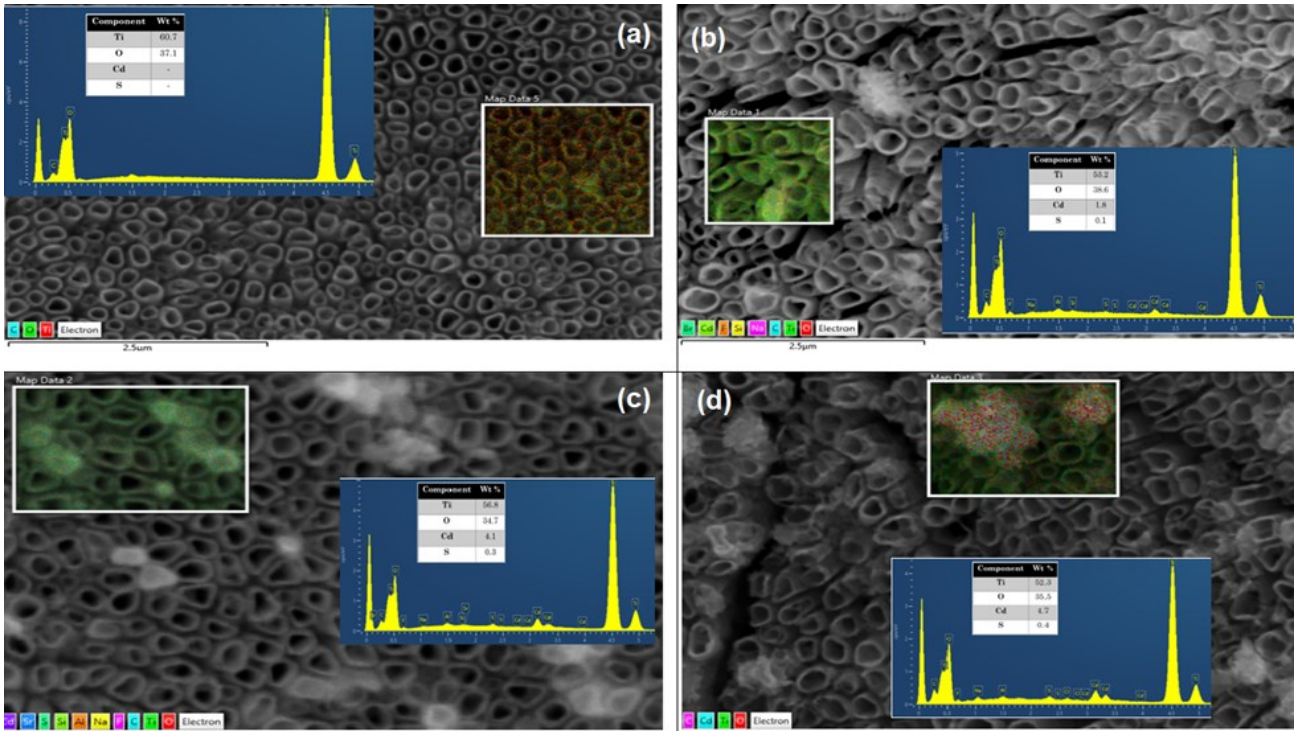

Figure 2. FE-SEM images with magnification of 20000X for (a) T; (b) CT 0.05; (c) CT 0.1; (d) CT 0.2.

6. Excess hydroxyl ion is obtained during the synthesis process, hence the adsorption of Cd^{2+} is higher than the S^{2-} [25].

The results of the Field Emission Scanning Electron Microscopy (FESEM) readings shown in Figure 2 show the distribution of Ti, O, Cd, and S components on the surface of the photocatalyst. It can be seen that Cd and S are concentrated in parts resembling white mist, although these components are also visible in other parts. A correlation between the precursor concentrations used during the synthesis of nanocomposites and the amount of CdS on the TNTA surface can also be seen. The size of the white mist on the surface of the nanotube tends to increase when the precursor concentration is more significant. Under certain conditions, the larger the size of the mist, which contains Cd and S, have a shading effect on TNTAs, thereby affecting the performance of TNTA in the photocatalytic process. This explains the effect of precursor concentration on the performance of CdS/TNTAs nanocomposites.

3.2 XRD Characterization

Figure 3 shows the peaks found at 2θ and matching the diffraction peaks of the anatase phase at (101), (200), (105), and (221) (JCPDS No. 21-1272) are 25.4°, 48.2°, 54.1°, and 55.2°. However, no CdS peak was detected because

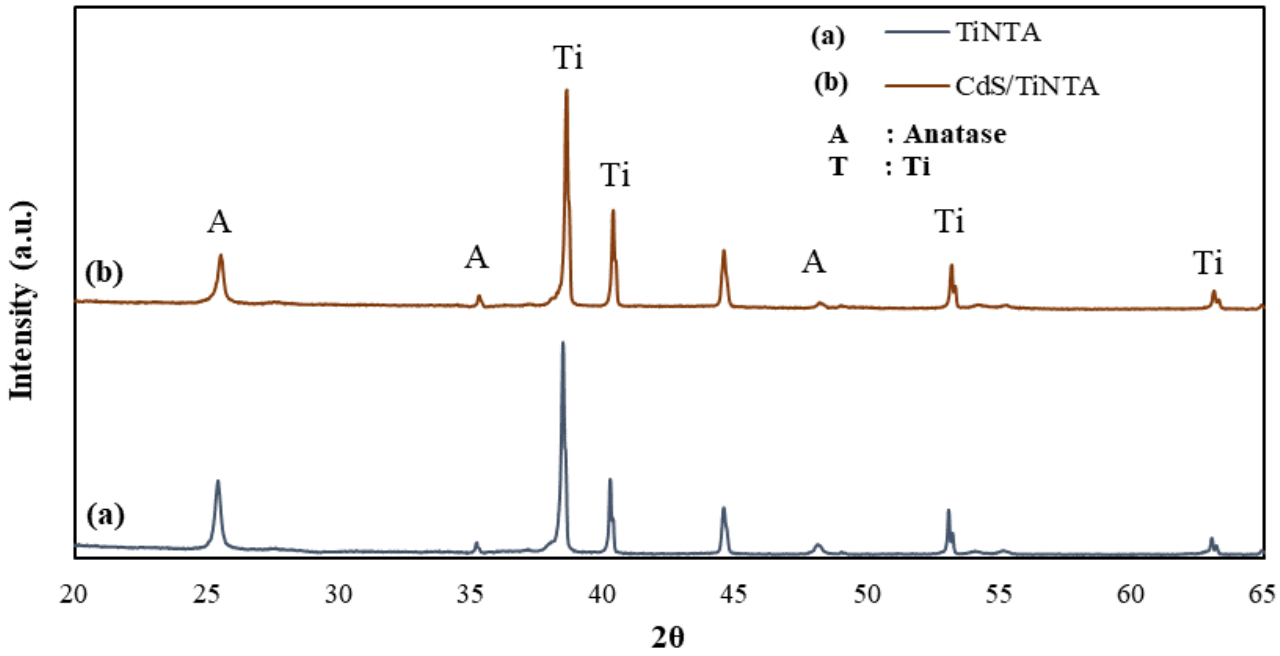

Figure 3. XRD patterns of TNTAs and CdS/TNTAs.

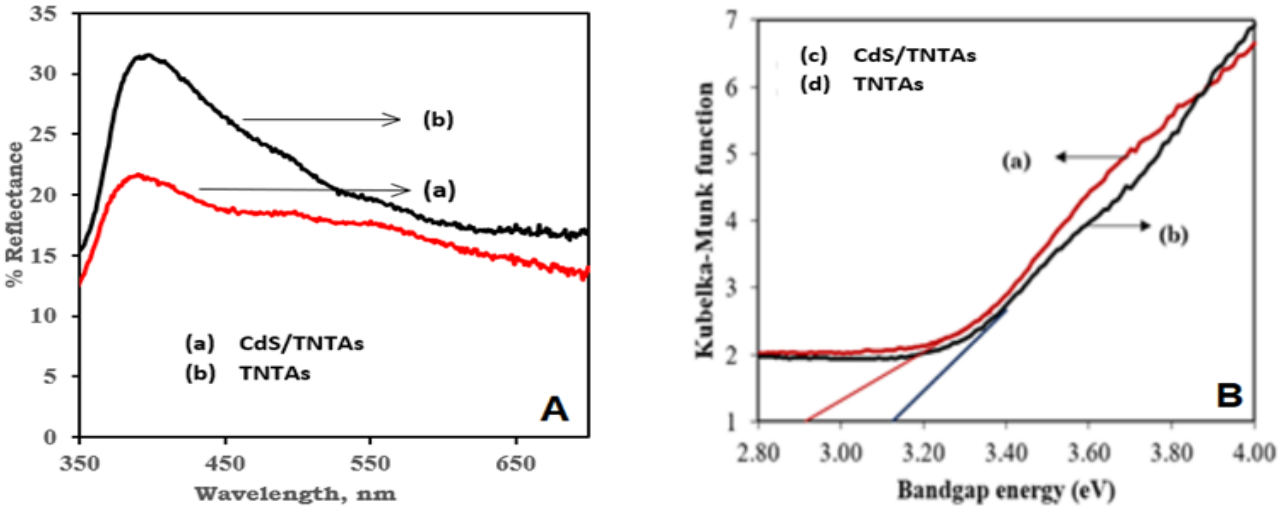

Figure 4. (A) Absorption behavior of UV-visible diffuse reflectance spectrum of photocatalysts, (B) Tauc plot of Kubelka-Munk equation.

the total amount was relatively low. No significant difference exists between the TNTAs XRD pattern and the modified CdS/TNTAs X-ray diffraction pattern. The slight shift and size of the anatase crystal peaks indicate the presence of CdS in TNTAs crystals. Furthermore, this is strengthened by FESEM readings which confirm the presence of CdS on the surface of the photocatalyst.

3.3 UV-Vis DRS Characterization

The photocatalyst bandgap of unmodified TNTAs and the CdS/TNTAs composites was estimated by establishing the Kubelka-Munk function and Tauc plot. The band gap energy resulted from the extrapolation of the linear portion of the Tau plot (F(R).hv) to the energy (HV) axis, as shown in Figure 4. Furthermore, the figure shows that the CdS/TNTAs composite lowers the bandgap energy of pure TNTAs from 3.16 eV to 2.92 eV. CdS extends the photon absorption towards the visible light area; hence, this photocatalyst exhibits enhancement in photoresponse under visible light.

3.4 Electrocoagulation-photocatalysis Test on Ciprofloxacin Degradation and Hydrogen Production

Ciprofloxacin degradation and hydrogen production are tested on three systems: electrocoagulation, photocatalysis, and electrocoagulation-photocatalysis. The ability of each system to remove pollutants and produce hydrogen is also compared.

3.4.1 Electrocoagulation test on ciprofloxacin removal and hydrogen production

Electrocoagulation is an electrochemical process in which an oxidation reaction occurs on the surface of the anode (aluminum), which then bind to hydroxyl ions to form a coagulant $Al(OH)_3$. The direct current voltage of 20 V used in the electrocoagulation test was based on the results from preliminary studies [16]. The reaction happened in an electrocoagulation process for the Ciprofloxacin removal:

$$Al \rightarrow Al^{3+} + 3e^- \quad (2)$$

$$Al^{3+} + 3(H^+ + OH^-) \rightarrow Al(OH)_3 + 3H^+ \quad (3)$$

$$Al(OH)_3 + C_{17}H_{18}FN_3O_3 \rightarrow \text{Pollutant Adsorption} \quad (4)$$

$$2H_2O + 2e^- \rightarrow 2OH^- + H_{2(g)} \quad (5)$$

According to research by Muttaqin *et al.* [16], the electrocoagulation process is carried out in an alkaline state because it produces abundant coagulants hence the absorption efficiency of dissolved pollutants is expected to be better. Additionally, the amount of hydrogen produced is more significant in the electrocoagulation process in the alkaline phase. Meanwhile, in chemical equilibrium, more hydroxyl ions form the coagulant, with a decrease in hydrogen ions to gas [16]. Figure 5 shows the electrocoagulation test result conducted for 4 hours, indicating that the removal of ciprofloxacin has an efficiency of 62.77% with a sediment mass of 0.4521 g and simultaneously produces hydrogen gas of 0.94 mol/m^2.

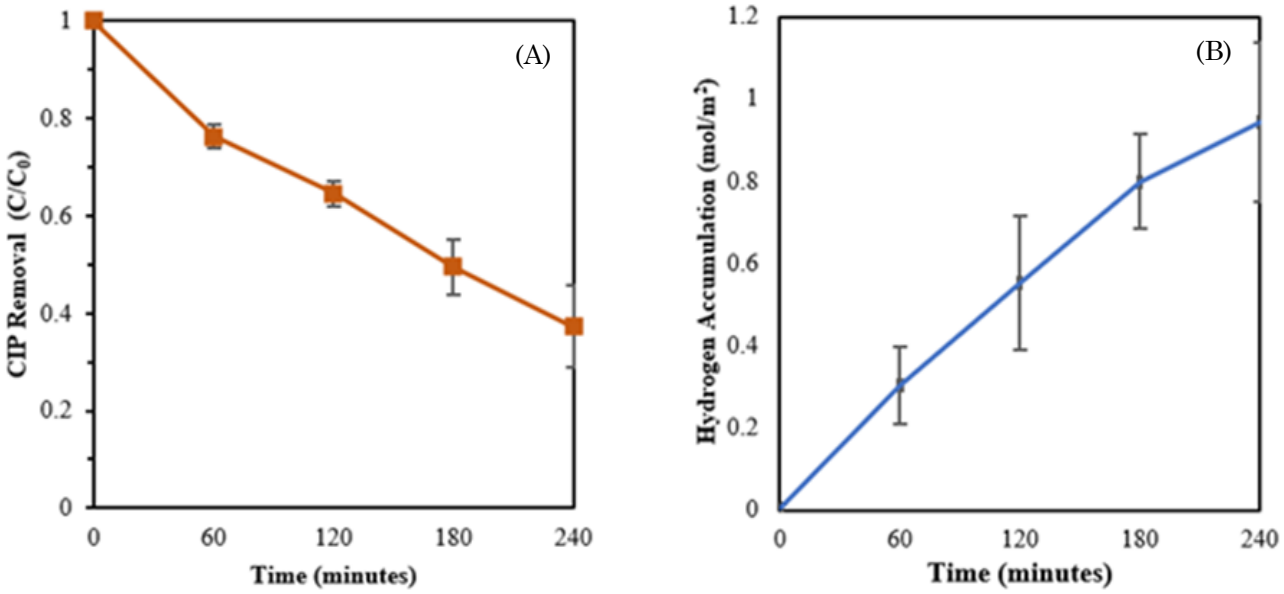

Figure 5. (A) CIP removal on electrocoagulation system; (B) Hydrogen accumulation.

3.4.2 Photocatalysis Test

The photocatalyst T, CT 0.5, CT 0.1, and CT 0.2 were tested to determine their ability to degrade ciprofloxacin and produce hydrogen simultaneously in a single photocatalysis system. Figure 6 shows that CT 0.05, CT 0.1, and CT 0.2 exhibit a better photocatalytic activity than T. This indicates that the composite formation of CdS/TiNTAs has successfully enhanced the photocatalytic performance of ciprofloxacin degradation and also hydrogen production.

Furthermore, Figure 6 shows that CT 0.1 exhibited the highest performance. From the trend, it can be concluded that the higher concentration of the precursor Cd^{2+} and S^{2-} can increase the photocatalytic activity. Wang *et al.* [13] study on Metronidazole degradation using CdS/TiO_2 evaluated the possible mechanism of ciprofloxacin degradation on CdS/TNTAs photocatalyst under visible light.

$$CdS + h\nu \rightarrow CdS\ (h_{VB}^{+} + e^{-}) \quad (6)$$

$$CdS\ (h_{VB}^{+} + e^{-}) + TiO_2 \rightarrow CdS(h_{VB}^{+}) + TiO_2(e_{CB}^{-}) \quad (7)$$

$$CdS(h_{VB}^{+}) + OH^{-} \rightarrow CdS + OH^{\bullet} \quad (8)$$

$$TiO_2(e_{CB}^{-}) + O_2 \rightarrow TiO_2 + O_2^{\bullet -} \quad (9)$$

$$O_2^{\bullet -} + e_{CB}^{-} + 2H^{+} \rightarrow H_2O_2 \quad (10)$$

$$O_2 + 2e_{CB}^{-} + 2H^{+} \rightarrow H_2O_2 \quad (11)$$

$$H_2O_2 + e_{CB}^{-} \rightarrow OH^{\bullet} + OH^{-} \quad (12)$$

$$O_2^{\bullet -}, H_2O_2, OH^{\bullet}, h_{VB}^{+}, \ldots + C_{17}H_{18}FN \rightarrow \text{Degraded Products} \quad (13)$$

The condition of the sample solution using water as a solvent allows the water splitting reaction to produce hydrogen according to the reaction:

$$TiO_2(e_{CB}^{-}) + 2H^{+} \rightarrow TiO_2 + H_2 \quad (14)$$

The combination and contact between TiO_2 and CdS provide space for electron transfer, photogeneration, and hole separation [26]. The position of the energy band gap of CdS which is responsive to visible light exposure, allows the incorporation of CdS and TiO_2 to expand the light spectrum capable of activating photocatalysts, as shown in the results of the UV-Visible DRS test. However, the most optimal photocatalytic activity was obtained when the CdS precursor concentration was added at 0.1 M to the TNTAs photocatalyst. Conversely, the photocatalyst's ability to degrade ciprofloxacin decreased when 0.2 M of the CdS precursor was added. This condition occurs because the excess CdS prevents photons from entering the TiO_2 surface; as shown in the FESEM results. Thus the limitations of the photon energy received result in not optimal process of excitation of electrons on the surface of the photocatalyst. Meng *et al.* [26] stated that the excessive addition of CdS reduces the active site of the TiO_2 photocatalyst, which is correlated with the decreased surface area exposed to the light source. Therefore, an appropriate concentration of CdS precursor is required to synthesize CdS/TiO_2 composites to obtain optimal photocatalytic activity.

3.4.3 Electrocoagulation-photocatalysis test

The highest performance of CT0.1 was used as the photocatalyst in the combination of the electrocoagulation and photocatalysis process to observe the activity of ciprofloxacin degradation and hydrogen production. The combined process was carried out in a reactor with a volume of 500 mL containing 10 ppm ciprofloxacin at pH 10, as shown in Figure 8. The integrated system was tested on varying voltages of 5 V,

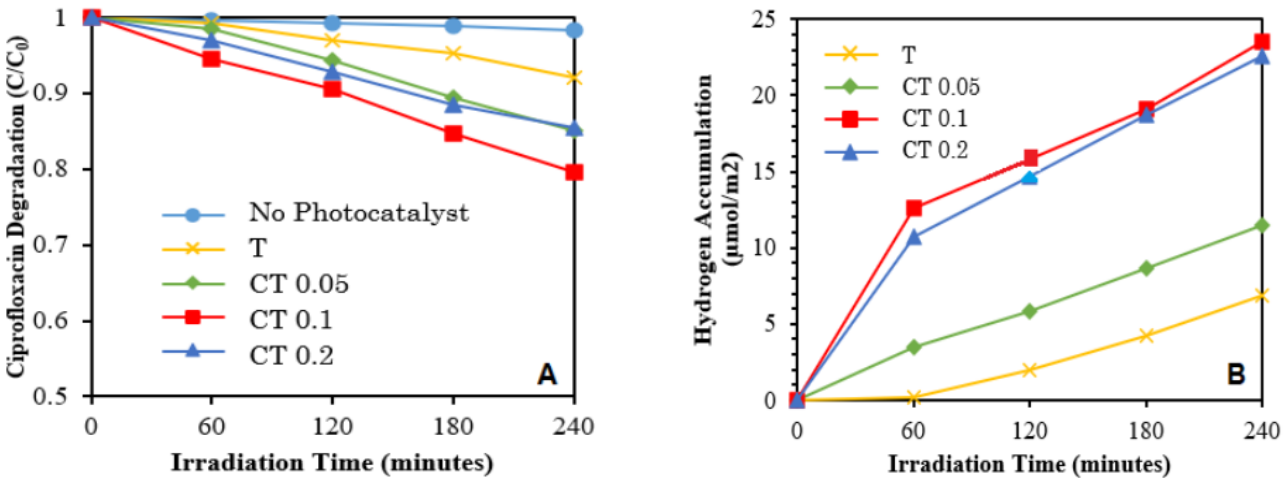

Figure 6. (A) CIP removal on photocatalysis system and (B) hydrogen accumulation.

10 V, and 20 V. Figure 7 shows that different voltages result in further pollutant degradation efficiency. The highest pollutant degradation efficiency was achieved at 86.55%, and the result showed that the bigger the voltage applied, the more the pollutant degraded. During the electrocoagulation process, the electric current flows through the anode and cathode following Ohm Law, which states that current is directly proportional to voltage. Therefore, when the voltage is increased, the amount of Al^{3+} ions also rises, with an increase in the adsorption of $Al(OH)_3$, more pollutants, and the formation of precipitating flocs, separated by the gas produced.

Figure 7(A) shows that the concentration of CIP decreased significantly during the initial process because the Al^{3+} solubility increased at the beginning of the reaction. Furthermore, the anode experienced passivation due to the presence of oxide ions on the electrode surface; hence the coagulant produced is less than that of the beginning process [27].

The same thing can also be observed in the amount of hydrogen produced in Figure 7(B), where the effect of voltage on hydrogen production and a combination of electrocoagulation and photocatalysis system is 0.85 mol/m², 1.3 mol/m², and 2.62 mol/m², respectively. In the

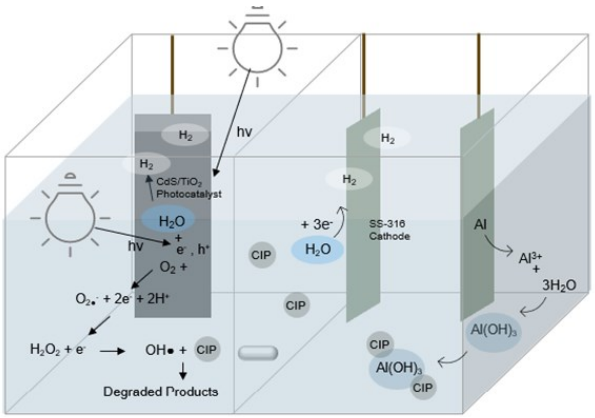

Figure 8. Illustration of the combined system of electrocoagulation and photocatalysis.

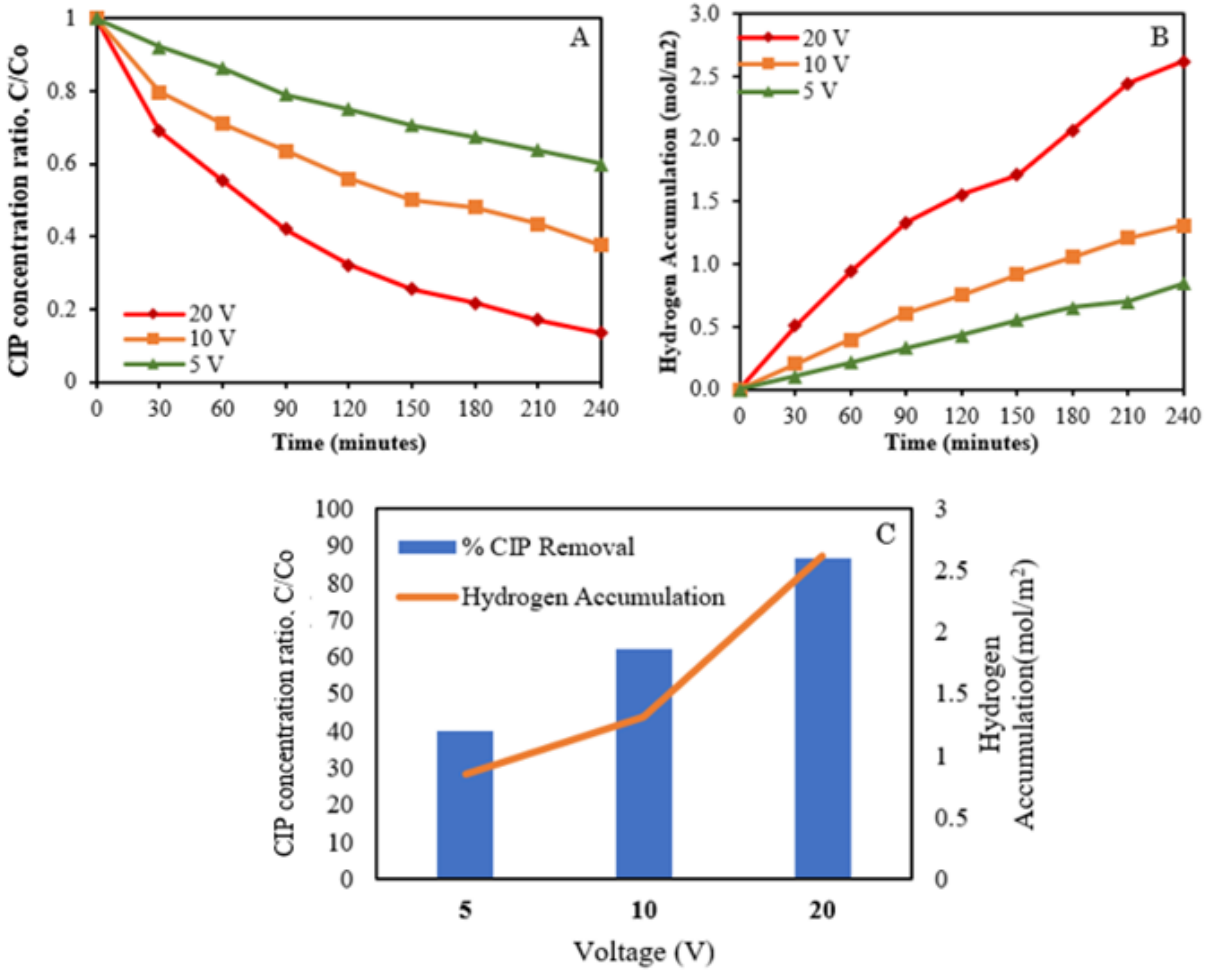

Figure 7. The effect of voltage in the performance of combined system (electrocoagulation and photocatalysis): (A) CIP concentration ratio, (B) Accumulation of hydrogen production, (C) Comparison the performance of process at various voltage.

combined electrocoagulation and photocatalysis system, Al is oxidized to Al^{3+}, followed by forming a coagulant with OH^- to become $Al(OH)_3$. According to preliminary studies, voltage affects the current in the electrocoagulation process, as shown in Figure 7(C). The higher the current, the greater the amount of Al^{3+} solution and more electrons. Therefore, the amount of H_2 produced increases as the voltage rises. Additionally, the reaction at the anode will shift to the right to produce more electrons due to the abundance of OH^- that reacts with Al^{3+}. The electrons produced from the oxidation of Al to Al^{3+} are also able to reduce H^+ ions and form hydrogen gas [16].

3.4.4 Comparison between electrocoagulation, photocatalysis, and electrocoagulation-photocatalysis using CdS/TiNTAs photocatalyst

Ciprofloxacin removal and hydrogen production tests were carried out on a combined electrocoagulation and photocatalysis (E-P combination) system using various voltages. The results showed that the system had the highest efficiency at a voltage of 20 V with a removal ciprofloxacin efficiency and hydrogen production of 86.55% and 2.62 mol/m² in 240 min, respectively. Figure 9(A) shows the comparative profile of ciprofloxacin removal in various processes, with higher efficiency obtained in the E-P combination system than the single photocatalytic and electrocoagulation. The efficiency of the photocatalysis, electrocoagulation and E-P combination systems are 20.43%, 62.57%, and 86.55%, respectively. The E-P combination system is proven to provide a synergistic effect to increase process efficiency.

The standard limit for ciprofloxacin before being released into the environment is 1 µg/L [28]. In the E-P combination system, the concentration of ciprofloxacin decreased by 86.55% from 10 ppm to 1.32 ppm within 240 min. However, the additional processing time is needed to reduce the concentration to the quality standard of 1 µg/L. The concentration of ciprofloxacin in a single electrocoagulation process decreased from 10 ppm to 3.75 ppm, which is 62.57% reduction for 240 min. Meanwhile, in the single photocatalysis process, the concentration of ciprofloxacin successfully decreased by 20.43% from 10 ppm to 7.71 ppm within 240 min.

Figure 9(B) shows that the accumulation of hydrogen from the E-P combination system is much higher when compared to the single electrocoagulation and photocatalytic systems. In the E-P combination, single electrocoagulation, and photocatalysis systems, the hydrogen accumulation obtained at 240 minutes consecutively were 2.6 mol/m², 0.94 mol/m², and 23.5 µmol/m². The hydrogen accumulation obtained from the E-P combination system increased to more than twice the accumulation produced from the single electrocoagulation system. This tends to occur because there is a synergistic effect between the two systems; hence more H^+ is used to produce H_2 gas. The application of a simultaneous process allows for the Le Cathelier's effect to occur between the reactions in the electrocoagulation process and in the photocatalytic process. This can be explained in the reactions (5) dan (8):

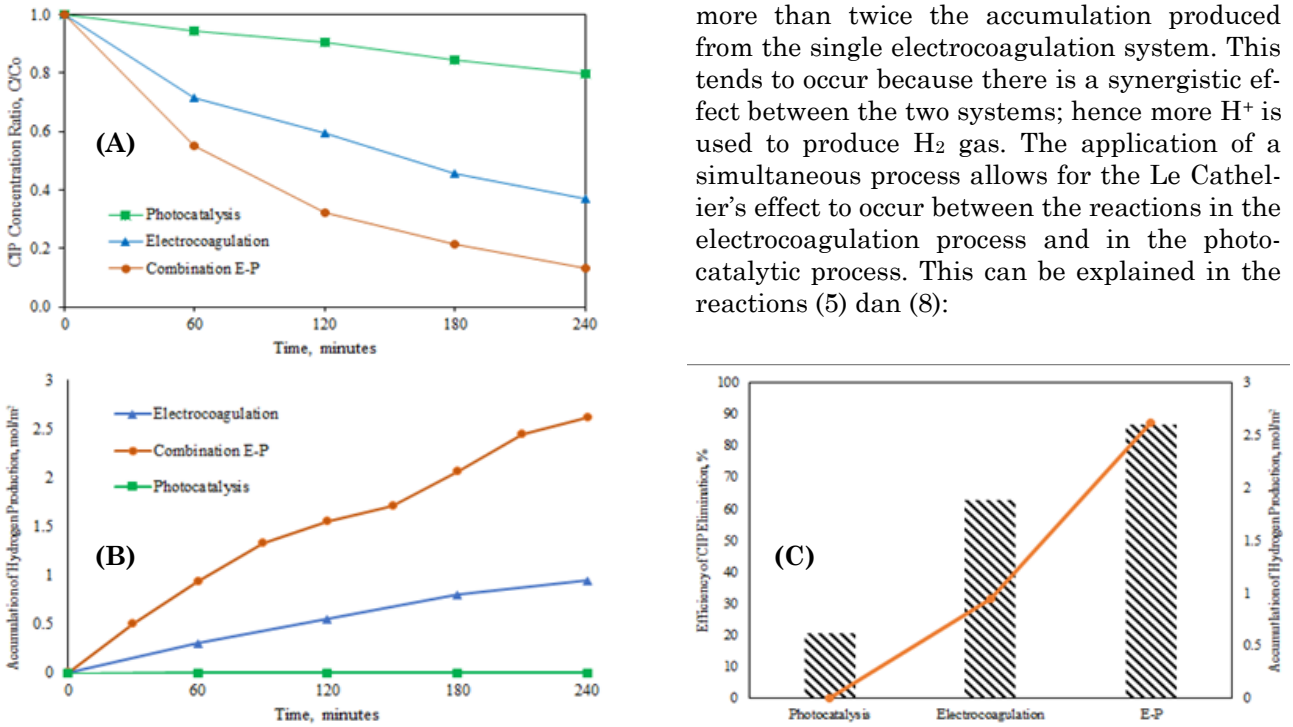

Figure 9. Comparison between single system of photocatalysis, electrocoagulation, and E-P combination: (A) CIP removal (B) hydrogen accumulation (C) CIP removal efficiency vs hydrogen accumulation.

Hydrogen production reaction in the electrocoagulation process :

$$2H_2O + 2e^- \rightarrow 2OH^- + H_{2(g)} \quad (5)$$

Oxydation reaction at valence band in the photocatalysis prosecess :

$$CdS(h_{VB}^+) + OH^- \rightarrow CdS + OH^\bullet \quad (8)$$

The H^+ and OH^- ions seen in the reaction are ions produced from water molecules because the system contains a ciprofloxacin solution with abundant water molecules. Equation (8) shows that the presence of holes on the photocatalyst surface conducts an oxidation reaction of $(OH)^-$. The more successfully the photocatalyst inhibits electron-hole recombination, and the more holes are available so that more $(OH)^-$ can be oxidized. The Le Chatelier effect is then seen when other reactions occur, such as reaction (5), where continuous consumption of $(OH)^-$ in reaction (8) shifts the equilibrium in reaction (5) to the right. These conditions mean that hydrogen gas production, according to reaction (5), increases.

Thus when a simultaneous process occurs, and the performance of the photocatalyst in suppressing the optimal electron-hole recombination rate, the production of hydrogen gas increases significantly. In addition, the success in suppressing the photocatalyst's recombination rate also affects the ability to eliminate the CIP content in the sample solution. When the recombination rate is optimally reduced, the availability of more holes increases the ability of the photocatalyst to degrade ciprofloxacin.

The E-P combination using 10 V power with a processing time of 240 min had the same ciprofloxacin removal ability as a single electrocoagulation system at 20 V with CIP efficiency removal of 62.36% and 62.57%, respectively. Meanwhile, the hydrogen gas produced in the E-P combination system at 10V was higher than the yield in the 20 V single electrocoagulation system, at 1.36 mol/m^2 and 0.94 mol/m^2, respectively. In conclusion, the combination of electrocoagulation-photocatalysis has a synergistic effect on increasing the efficiency of ciprofloxacin removal and the simultaneous production of hydrogen.

This analysis follows several preliminary studies on the hydrogen yield from ciprofloxacin wastewater treatment at values of 0.0544 mmol/g/h and 2.725 mmol/g/h [29]. The accumulation of hydrogen from the simultaneous degradation of ciprofloxacin in the E-P combination process has a much higher amount of 2.6 mol/m^2 for 240 min or 0.65 mol/m^2/h [30]. In addition, using ciprofloxacin wastewater as a sacrificial agent in producing hydrogen is an alternative to the difficulty of using water as raw material for fuel cells to produce pure hydrogen from the electrolysis process.

4. Conclusions

In conclusion, composite 0.1 M CdS/TiNTAs (CT 0.1) has the most optimal photocatalytic activity with the ability to degrade ciprofloxacin by 20.43% and simultaneous hydrogen production of 23.5×10^{-6} mol/m^2. The SEM characterization and the EDX spectrum confirmed the presence of nanotubular morphology and Cd -S composites. The CdS/TNTAs nanocomposite synthesis produced a photocatalyst with an energy band gap of 2.92 eV without changing the crystallinity of the nanocomposite, as evidenced by XRD assays. The combined electrocoagulation and photocatalysis system (E-P combination) conducted using 0.1 M CdS/TiNTAs operated optimally at 20 V with 86.55% ciprofloxacin removal and hydrogen production of 2.6 mol/m^2 within 240 min. The E-P combination process increased the degradation ability of ciprofloxacin by 24% and 66% against the single electrocoagulation or photocatalytic systems. The E-P combination also increased hydrogen production by 2.8 times compared to the single electrocoagulation system at 20 V, which is much higher than the single photocatalysis system of 110 thousand times.

Acknowledgment

This project was financially supported by the program of PUTI Pascasarjana 2022 with Contract Number: NKB-343/UN2.RST/HKP.05.00/2022.

Credit Author Statement

Author contribution: R.L. Sugihartini: validation, formal analysis, investigation, data curation, writing original draft, visualization; R. Pratiwi: methodology, formal analysis, resources, investigation, writing-review, and editing; Slamet: conceptualization, writing-review and editing, supervision, project administration, funding acquisition. All authors have read and agreed to the published version of the manuscript.

References

[1] Kraupner, N., Ebmeyer, S., Bengtsson-Palme, J., Fick, J., Kristiansson, E., Flach, C.-F., Larsson, D.J. (2018). Selective concentration for ciprofloxacin resistance in Escherichia coli grown in complex aquatic bacterial biofilms. *Environment International,* 116, 255-268. DOI: 10.1016/j.envint.2018.04.029.

[2] Rodriguez-Narvaez, O.M., Peralta-Hernandez, J.M., Goonetilleke, A., Bandala, E.R. (2017). Treatment technologies for emerging contaminants in water: A review. *Chemical Engineering Journal,* 323, 361-380. DOI: 10.1016/j.cej.2017.04.106.

[3] Antonin, V.S., Santos, M.C., Garcia-Segura, S., Brillas, E. (2015). Electrochemical incineration of the antibiotic ciprofloxacin in sulfate medium and synthetic urine matrix. *Water Research, 83*, 31-41. DOI: 10.1016/j.watres.2015.05.066.

[4] Melián, E.P., Díaz, O.G., Méndez, A.O., López, C.R., Suárez, M.N., Rodríguez, J.M.D., Navío, J.A., Hevia, D.F., Peña, J.P. (2013). Efficient and affordable hydrogen production by water photo-splitting using TiO_2-based photocatalysts. *International Journal of Hydrogen Energy,* 38(5), 2144-2155. DOI: 10.1016/j.ijhydene.2012.12.005.

[5] Al-Mamun, M., Kader, S., Islam, M., Khan, M. (2019). Photocatalytic activity improvement and application of UV-TiO_2 photocatalysis in textile wastewater treatment: A review. *Journal of Environmental Chemical Engineering,* 7(5), 103248. DOI: 10.1016/j.ijhydene.2018.10.200

[6] Fajrina, N., Tahir, M. (2019). A critical review in strategies to improve photocatalytic water splitting towards hydrogen production. *International Journal of Hydrogen Energy,* 44(2), 540-577. DOI: 10.1016/j.ijhydene.2018.10.200.

[7] Lin, Y., Jiang, Z., Zhu, C., Hu, X., Zhu, H., Zhang, X., Fan, J., Lin, S.H. (2013). The optical absorption and hydrogen production by water splitting of (Si, Fe)-codoped anatase TiO_2 photocatalyst. *International Journal of Hydrogen Energy,* 38(13), 5209-5214. DOI: 10.1016/j.ijhydene.2013.02.079.

[8] Ratnawati, J.G., Dewi, E., Slamet, S. (2014). Effect of NaBF4 addition on the anodic synthesis of TiO_2 nanotube arrays photocatalyst for production of hydrogen from glycerolwater solution. *International Journal of Hydrogen Energy,* 39(30), 16927-16935. DOI: 10.1016/j.ijhydene.2014.07.178.

[9] Wang, W.-Y., Chen, B.-R. (2013). Characterization and photocatalytic activity of TiO_2 nanotube films prepared by anodization. *International Journal of Photoenergy*, 2013, 348171. DOI: 10.1155/2013/348171

[10] Parvulescu, V., Ciobanu, M., Petcu, G. (2020). Immobilization of semiconductor photocatalysts. In *Handbook of smart photocatalytic materials* (pp. 103-140): Elsevier. DOI: 10.1016/B978-0-12-819051-7.00004-X

[11] Huang, F., Yan, A., Zhao, H. (2016). Influences of doping on photocatalytic properties of TiO_2 photocatalyst. In Cao, W. (ed.), *Semiconductor Photocatalysis—Materials, Mechanisms and Applications*, p. 31-80, IntechOpen. DOI: 10.5772/63234.

[12] Kumaravel, V., Mathew, S., Bartlett, J., Pillai, S.C. (2019). Photocatalytic hydrogen production using metal doped TiO_2: A review of recent advances. *Applied Catalysis B: Environmental,* 244, 1021-1064. DOI: 10.1016/j.apcatb.2018.11.080.

[13] Wang, P., Xu, S., Wang, J., Liu, X. (2020). Photodeposition synthesis of CdS QDs-decorated TiO_2 for efficient photocatalytic degradation of metronidazole under visible light. *Journal of Materials Science: Materials in Electronics,* 31(22), 19797-19808. DOI: 10.1007/s10854-020-04504-2.

[14] Sharfan, N., Shobri, A., Anindria, F.A., Mauricio, R., Tafsili, M.A.B., Slamet, S. (2018). Treatment of batik industry waste with a combination of electrocoagulation and photocatalysis. *International Journal of Technology*. 9(5), 936-943. DOI: 10.14716/ijtech.v9i5.618

[15] Pelawi, L. F., Slamet, S., & Elysabeth, T. (2020). Combination of electrocoagulation and photocatalysis for hydrogen production and decolorization of tartrazine dyes using CuO-TiO_2 nanotubes photocatalysts. *AIP Conference Proceedings*, 2223, 040001. DOI: 10.1063/5.0000953.

[16] Muttaqin, R., Pratiwi, R., Dewi, E.L., Ibadurrohman, M. (2022). Degradation of methylene blue-ciprofloxacin and hydrogen production simultaneously using combination of electrocoagulation and photocatalytic process with Fe-TiNTAs. *International Journal of Hydrogen Energy,* 47(42), 18272-18284. DOI: 10.1016/j.ijhydene.2022.04.031.

[17] Dholam, R., Patel, N., Adami, M., Miotello, A. (2009). Hydrogen production by photocatalytic water-splitting using Cr-or Fe-doped TiO_2 composite thin films photocatalyst. *International Journal of Hydrogen Energy,* 34(13), 5337-5346. DOI: 10.1016/j.ijhydene.2009.05.011.

[18] Ahmadzadeh, S., Asadipour, A., Pournamdari, M., Behnam, B., Rahimi, H.R., Dolatabadi, M. (2017). Removal of ciprofloxacin from hospital wastewater using electrocoagulation technique by aluminum electrode: optimization and modelling through response surface methodology. *Process Safety and Environmental Protection,* 109, 538-547. DOI: 10.1016/j.psep.2017.04.026.

[19] Naje, A.S., Chelliapan, S., Zakaria, Z., Ajeel, M.A., Alaba, P.A. (2017). A review of electrocoagulation technology for the treatment of textile wastewater. *Reviews in Chemical Engineering,* 33(3), 263-292. DOI: 10.1515/revce-2016-0019.

[20] Boroski, M., Rodrigues, A.C., Garcia, J.C., Sampaio, L.C., Nozaki, J., Hioka, N. (2009). Combined electrocoagulation and TiO_2 photoassisted treatment applied to wastewater effluents from pharmaceutical and cosmetic industries. *Journal of Hazardous Haterials,* 162(1), 448-454. DOI: 10.1016/j.jhazmat.2008.05.062.

[21] Ates, H., Dizge, N., Yatmaz, H.C. (2017). Combined process of electrocoagulation and photocatalytic degradation for the treatment of olive washing wastewater. *Water Science and Technology,* 75(1), 141-154. DOI: 10.2166/wst.2016.498.

[22] Afroz, K., Moniruddin, M., Bakranov, N., Kudaibergenov, S., Nuraje, N. (2018). A heterojunction strategy to improve the visible light sensitive water splitting performance of photocatalytic materials. *Journal of Materials Chemistry A*, 6(44), 21696-21718. DOI: 10.1039/C8TA04165B.

[23] Wang, J., Wang, Z., Qu, P., Xu, Q., Zheng, J., Jia, S., Chen, J., Zhu, Z. (2018). A 2D/1D TiO2 nanosheet/CdS nanorods heterostructure with enhanced photocatalytic water splitting performance for H_2 evolution. *International Journal of Hydrogen Energy,* 43(15), 7388-7396. DOI: 10.1016/j.ijhydene.2018.02.191.

[24] Momeni, M., Mozafari, A. (2016). The effect of number of SILAR cycles on morphological, optical and photo catalytic properties of cadmium sulfide–titania films. *Journal of Materials Science: Materials in Electronics,* 27(10), 10658-10666. DOI: 10.1007/s10854-016-5163-4.

[25] Kalarivalappil, V., Hinder, S.J., Pillai, S.C., Kumar, V., Vijayan, B.K. (2018). Stability studies of CdS sensitized TiO_2 nanotubes prepared using the SILAR method. *Journal of Environmental Chemical Engineering,* 6(1), 1404-1413. DOI: 10.1007/s10854-016-5163-4.

[26] Meng, A., Zhu, B., Zhong, B., Zhang, L., Cheng, B. (2017). Direct Z-scheme TiO_2/CdS hierarchical photocatalyst for enhanced photocatalytic H2-production activity. *Applied Surface Science,* 422, 518-527. DOI: 10.1016/j.apsusc.2017.06.028.

[27] Hakizimana, J.N., Gourich, B., Chafi, M., Stiriba, Y., Vial, C., Drogui, P., Naja, J. (2017). Electrocoagulation process in water treatment: A review of electrocoagulation modeling approaches. *Desalination,* 404, 1-21. DOI: 10.1016/j.desal.2016.10.011.

[28] Sahlin, S., Larsson, D., Ågerstrand, M. (2018). Ciprofloxacin. EQS data overview. Department of Environmental Science and Analytical Chemistry (ACES). *ACES report*(15).

[29] Wu, S., Hu, Y.H. (2021). A comprehensive review on catalysts for electrocatalytic and photoelectrocatalytic degradation of antibiotics. *Chemical Engineering Journal,* 409, 127739. DOI: 10.1016/j.cej.2020.127739.

[30] Wu, X., Zhang, Y., Wu, H., Guo, J., Wu, K., Zhang, L. (2021). Facile synthesis of multi-shelled AgI/ZnO composite as Z-scheme photocatalyst for efficient ciprofloxacin degradation and H_2 production. *Journal of Materials Science: Materials in Electronics,* 32(22), 26241-26257. DOI: 10.1007/s10854-021-06844-z.